

Article

# Design, Manufacture and Performance Test of the Thermoelectric Generator System for Waste Heat Recovery of Engine Exhaust

Tzer-Ming Jeng <sup>†</sup>, Sheng-Chung Tzeng <sup>\*,†</sup>, Bo-Jun Yang and Yi-Chun Li

Received: 26 November 2015; Accepted: 5 January 2016; Published: 11 January 2016

Academic Editor: Chien-Hung Liu

Department of Mechanical Engineering, Chienkuo Technology University, Changhua City 500, Taiwan; tmjeng@cc.ctu.edu.tw (T.-M.J.); jordan12873@yahoo.com.tw (B.-J.Y.); iancool1255@yahoo.com.tw (Y.-C.L.)

\* Correspondence: tsc@ctu.edu.tw; Tel.: +886-4-711-1111 (ext. 3190); Fax: +886-4-713-5677

† These authors contributed equally to this work.

**Abstract:** This study integrated the techniques of the high-performance heat transfer and thermoelectric conversion to build a thermoelectric generator system installed at the exhaust pipe of a real single-cylinder and four-stroke engine of 35.8 c.c. displacement. This system was made of the heat absorber, thermoelectric generator modules and the external heat sink. The pin-fin array was inserted into the circuitous duct to form the heat absorber, which could increase the heat-exchange surface area and the heat-exchange time to reach the object of absorbing heat and increasing thermoelectric conversion effectively.

**Keywords:** heat recovery; thermoelectric generator system; heat absorber of pin-fin array

## 1. Introduction

Thermoelectric conversion was discovered towards the end of the 19th century. Electrons are capable of carrying heat, as well as electricity. When a temperature difference exists between the two end faces of a thermoelectric material, many electrons will travel from the hot end face to the cold one. This phenomenon is known as the Seebeck effect and forms the basis on which the thermoelectric generation module was developed. As we are all aware, the global energy crisis is becoming worse and much emphasis is being placed on environment protection and the recovery of energy resources. These include waste heat from cooling water, exhaust gas, and steam power plants, amongst others. TEG modules are light and silent, have no moving parts and can convert recycled heat directly into electricity.

Champier *et al.* [1] pointed out that developing countries are currently using massive bio-fuel furnaces to mitigate global warming. The efficiency of these bio-fuel furnaces has been significantly improved in laboratory prototypes which give better combustion efficiency and produce less pollution. TEGs have been installed in them and the electricity generated can be used for lighting or to power circulation fans to improve the fuel-air ratio which, in turn, results in more complete combustion. Experiments were first carried out to verify the thermoelectric conversion ratio of a Bi<sub>2</sub>Te<sub>3</sub> TEG module and then the feasibility of combining the TEG module with a bio-fuel furnace and determination of the optimal position for installation was studied. Finally it was demonstrated that 6 W could be generated by thermoelectric conversion. Karri *et al.* [2] studied the efficiency of waste heat electricity generation using thermoelectric conversion in two practical cases: a sport utility vehicle (SUV) and a compressed natural gas (CNG)-fueled generator engine. Two different thermoelectric modules (available on the market) were used: (1) bismuth telluride (Bi<sub>2</sub>Te<sub>3</sub>), and (2) quantum-well (QW) device. Tests of the CNG engine and the SUV under the same conditions and the same generated AC output, showed the

QW device to be more efficient than the  $\text{Bi}_2\text{Te}_3$  TEG. In other words, more electricity was generated from the same amount of heat and more fuel was saved. Zhou *et al.* [3] pointed out that because water is a good heat conductor, combining commercial water heaters with thermoelectric modules in a thermoelectric conversion generator system was a good idea. They employed Carnot efficiency and the Coupled Physical Energy Balance Method that combines Joule heating, with the Seebeck, Peltier, and Thomson effects to predict the efficiency of a thermoelectric conversion generator system. Thirty different configurations involving a number of parameters were investigated, these included: the water flow model, hot water inlet temperature, pressure drop, cross-sectional area of the duct, duct length, the number of ducts, and so on. Systematic analysis showed that the upper modules would rival the upstream module in heat absorption, resulting in a lower temperature difference between the two faces of the thermoelectric module. They also pointed out that reducing coverage by modules in the downstream of an exhaust duct might result in its wall temperature being higher than the temperature of the hot-face of the upstream modules, which offers an opportunity to maximize overall power generation. Wang and Huang [4] investigated the conversion of vehicle engine exhaust heat to electrical power using thermoelectric generator modules. They employed numerical simulation to analyze multiple thermoelectric modules attached to heat exchanger surfaces in a series arrangement. They found that using more modules did not necessarily generate more power, and that the average generation ratio of each module actually decreased as the number of modules rose. The reason for this was that the temperature of the exhaust duct wall decreased rapidly along the direction of flow and this resulted in poor performance by the downstream TEGs. Jang and Tsai [5] considered attaching multiple TEG modules on stacked wall faces and found the amount of unit area generation was strongly affected by the spacing of the modules. Their thermoelectric generator configuration consisted of thermal plates (a stack wall), heat distribution plates, TEG modules, and water-cooled cooling plates. They used limited element analysis to simulate the overall thermoelectric conversion of the modules with different spacing and also with different thickness of heat distribution plates. The variable operation parameters included the temperature difference between the hot exhaust gas and the cooling water ( $\Delta T = 200\text{--}800$  K) and heat conductance coefficient of the heat distribution plate ( $h = 20\text{--}80$  W/m<sup>2</sup>/K). The aim of the simulation was determination of the optimal spacing between modules and the ideal thickness of heat distribution plates that gave the maximum generation per unit area. It has become clear that as the conversion efficiency of TEG material has increased so has the attention being paid to studies and applications involving combinations of TEG modules and waste heat sources from both domestic and industrial activity. These include heat from vehicle engine exhausts, cooling water circulation systems in vehicle engines, generators using internal combustion engines, waste heat gas stacks, bio-fuel furnaces, ground heat from hot springs, *etc.* These many heat sources can provide suitable environments for thermoelectric modules that generate power using differential temperatures. With proper cooling, the temperature difference between the cold and hot sides of TEG modules can be raised to achieve ideal power generation.

Many current studies have addressed waste heat recovery from engines using TEG devices and many have claimed patents. Most studies on thermoelectric generation by the recovery of engine waste heat emphasize integrated thermo-electric conversion devices and performance simulations involving vehicle systems. A patent filed by Cumming [6] claimed that power can be generated and saved in batteries using a thermoelectric semi-conductor installed on the outside of an engine exhaust pipe used for driving a hybrid vehicle. A patent filed by Handa and Nagoya [7] involved the adding of an insulator on both the heated and cooled faces of a TEG module to widen the temperature difference between the faces and give better generation efficiency. Shinohara *et al.* [8] invented an electronic power supply control system that utilizes a thermoelectric device to generate electric power from exhaust gas as a secondary system generator. After a summary of applications, Rowe [9] pointed out that thermoelectric conversion systems using temperatures above 140 °C are commercially competitive. Hendricks and Lustbader [10] analyzed systems using waste heat thermoelectric conversion systems on medium and high power vehicles and found that they were capable of generating 5–6 kW power.

However, there are three technical impediments to the achievement of a high-performance system: the thermoelectric conversion system itself, optimal integration with the vehicle, and design of the thermoelectric interface. A study team at the Ohio State University accomplished waste heat recovery using a thallium-doped lead telluride thermoelectric module [11], which characterizes a thermoelectric effect. Heating up one end of the material will cause the electrons to move to the colder end, therefore generating electrical current. If used on vehicles, waste heat from the vehicle can be converted into electricity and fed back to the vehicle for re-use. Jeng *et al.* [12] investigated the performance of a heat absorber made of packed brass beads in a thermoelectric conversion system. This packed bead heat absorber was installed in a square channel and various flow orientations, both straight and jet, were investigated as well as the ratio of channel width to bead diameter. Their studies showed the local and average heat transfer characteristics for several parameters and can be used as a basis for the design of a novel porous heat absorber for thermoelectric conversion systems.

This study establishes an initial performance test platform for thermoelectric modules, examines the relationships between the external load resistance and the output voltage/current of the TEG and investigates the influence of temperature difference between the hot and cold faces and their average against maximum power generation. Using high-temperature exhaust gas from an actual 35.8 c.c. engine as the heat source and a patent applied for by the authors [13] as the blueprint, a complete thermoelectric conversion system (including heat absorber, thermoelectric generation module and heat sink) was constructed. The experiments were conducted under controlled laboratory conditions and careful measurements of the displacement of the engine, operation speed, temperature, and composition of the high temperature exhaust gas were made. The effects of the installation position of the thermoelectric conversion system and the corresponding external cooling airflow were studied and the results may be used as important references for the future design of vehicle thermoelectric conversion systems.

## 2. Experimental Method

### 2.1. Design of Waste Heat Recovery Thermoelectric Conversion System

A thermoelectric conversion system normally consists of heat absorbers, TEG modules, and heat sinks, where heat absorbers function as heat collectors to heat up the TEG, and the heat sink functions to dissipate heat from the cold end of the TEG module as rapidly and efficiently as possible to widen the temperature difference between the hot and cold faces, to enhance performance of the TEG module. The thermoelectric conversion heat recovery device constructed for this study is illustrated in Figure 1. The pin-fin heat absorber is situated inside the duct and the exhaust gases are guided along a circuitous path from the inlet across them as can be seen in Figure 1. The absorbed heat is conducted to the hot face of the TEG modules which are bolted to the surface of the heat absorbers. The exhaust gases are forced past the pin-finned heat absorbers and the resulting turbulence enhances heat exchange between the hot exhaust gases and the extensive surface of the heat exchangers. The device also acts as a silencer and reduces the noise of the engine. The parts are anodized to protect them from corrosion and this also improves their aesthetic appearance. The fin pins are all the same length and make contact with the baffle box in the center of the chamber. This arrangement guides the flow so that it is impossible for the exhaust gasses to get to the outlet without the development of turbulence and close contact with the large heat exchange surfaces on all four sides of the chamber, see Figure 1. The bases of the finned heat exchange units are fastened to the body of the device with machine screws. The TEG modules are clamped between the top of the heat exchangers and the cooling heat sinks, also with machine screws. This arrangement effectively stays the hot waste gas and achieves massive heat exchange. Figure 1 also shows an assembled heat exchange device with one heat exchanger block, TEG and cooling fin assembly removed for clarity. In use, the outer housing has four heat exchange blocks bolted to it and the ends of the heater exchange pins make contact with the central baffle box which acts to guide the hot gasses on the proper path across all the heat exchange surfaces to the outlet.

All the components, the heat absorbers, heat sinks, aluminum housing, and central baffle, are made of aluminum alloy and have been anodized.

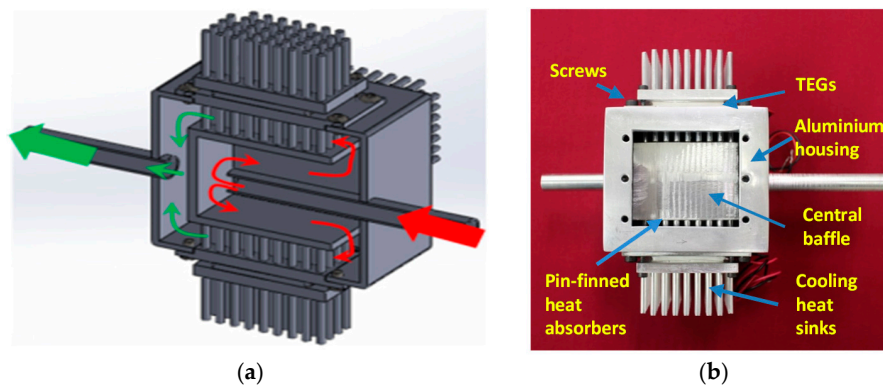


**Figure 1.** The thermoelectric conversion device used herein. (a) Cross-sectional view; (b) Photo of prototype.

2.2. Generation Performance Test of a Single-Chip TEG Module

The experimental setup for generation performance test of a single chip TEG module was shown in Figure 2. The setup includes (1) an air supply system; (2) a TEG module; (3) a test section (heating and cooling devices); and (4) the data acquisition equipment. The air supply for cooling the cold side of the TEG module was provided by an air compressor. The compressed air was stored in an 800 L tank to ensure a steady and pulse-free supply. The air flow was passed through a dryer and filter to remove water and impurities and an electronic controller (SIN-DP) was used to regulate the air flow which was guided to the cooling device of the test section. Air flow rates of 350–450 L/min were used for cooling the heat sink of cooling device, and then the temperature differences between the hot and cold faces of the TEG module were controlled to be 80, 100 and 120 °C.

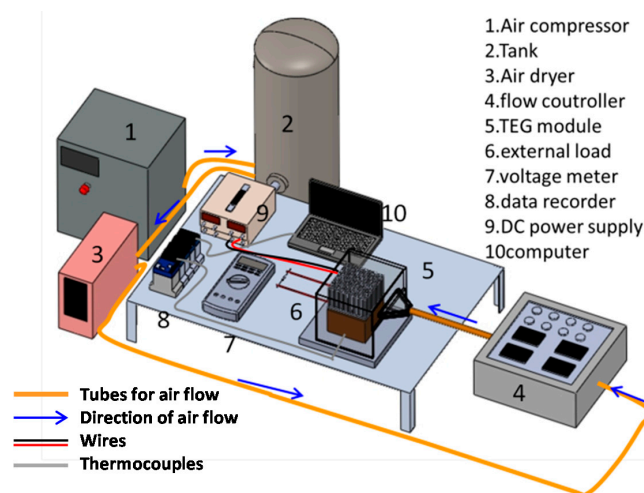


**Figure 2.** Experimental setup for the single-chip thermoelectric module experiment.

As shown in Figure 3, the TEG used in this experiment was manufactured by Russian Kryotherm (Model: TGM-287-1.0-1.5; dimensions: 40 mm × 40 mm × 3.8 mm). Figure 4 shows the present test section. In this experiment, the hot side of the TEG module was fastened to the heater using thermal grease. The heater was made of Bakelite (85 mm × 85 mm × 65 mm) with a stainless steel heating element (40 mm × 40 mm) and was powered by a DC power supply. The cold side of the TEG module was fastened by thermal grease to an aluminum alloy heat sink with an array of round pin



TT-T-30SLE T-Type thermocouples were embedded in the center of both the cold and hot faces of TEG module. Differential potential signals were retrieved by a YOKOGAWA MX-100 data recorder and converted into temperature readings. The TEG was connected to an external resistor load and the output voltage was measured by a multi-meter in parallel with the circuit. Power generated by the TEG module can be calculated using the voltage and resistor values. All data readings for computer processing were made at thermal equilibrium condition, when temperature fluctuation was less than 0.2 °C over 15 min.

The main target parameter of the experiment was generated power ( $P$ ) which was measured using voltage values with resistors of different values connected in series to the external circuit. The formula for the calculation of TEG power generation is:

$$P = V^2/R \quad (1)$$

where  $V$  stands for voltage,  $R$  for load resistance.

### 2.3. Generation Performance Test of the Thermoelectric Conversion System for a Real Engine

This experiment investigated power generation by a TEG system installed on the exhaust pipe of a 38.5 c.c. four-stroke engine. Figure 6 shows the layout used in this experiment, the equipment used includes (1) the engine; (2) the TEG conversion system; (3) an external air source (fan); and (4) the data acquisition system. The high-temperature exhaust gases from engine operation were guided through the thermoelectric conversion device in a way that ensures that maximum heat exchange took place. The thermoelectric conversion system, as shown in Figure 7, includes (1) the heat absorber; (2) the TEG modules; (3) the heat sinks; (4) the aluminum-alloy duct and other fittings. As the engine exhaust gases flowed through the duct, the internal heat absorber of pin-fin arrays conveyed heat rapidly to their external surface to which the TEG modules were fixed by machine screws and thermal grease. The other side (cold side) of each TEG was fastened in the same way to an outer heat sink. The substantial temperature difference between heat absorber and heat sink resulted in the efficient conversion of thermal energy into electricity. Figure 8 shows the assembled thermoelectric conversion system, an exploded diagram of the components, and the dimensions of the aluminum alloy duct. The heat absorber was made of 6061 aluminum alloy, and the configuration is shown in Figure 9. The heat sinks were made by extrusion from 6061 aluminum alloy and had evenly spaced rows of pin fins on the surface as shown in Figure 10. The four TEG modules used on the device were connected in series. The thermal grease was applied to the contact surfaces to ensure good heat conduction between the TEG surfaces and the heat absorber as well as heat sink. A fan drove air across the front of the engine, to simulate the oncoming air flow of a moving vehicle, and cooled the thermoelectric conversion system. The data acquisition system monitored and recorded the relevant temperatures, rotation speed, air flow rate, and the voltage and power outputs in real time. A K-type thermocouple was located at the inlet and outlet of the aluminum-alloy duct with built-in heat absorber. Thermocouples were also embedded between the TEG modules and heat-absorber plates as well as the TEG modules and the heat sinks. A one-point T-type thermocouple was embedded at the fan outlet. Measurements of the voltage generated by the TEGs were monitored by a micro-voltmeter in real time. The output of the thermocouples was measured through a data recorder and sent to the PC for real time analysis and recording. The speed of cooling air delivered by the fan was measured at the fan outlet and downstream of the test section using the airflow meter. The mean velocity ( $U$ ) of air passing through the heat sink was estimated based on the average value of the air speeds measured at these two positions. Engine rotation speed, controlled by the throttle valve, was measured by a tachometer.

The accuracy of measurements made during engineering tests of this kind is always affected by unpredictable factors. These may be physical and connected with the equipment, or may be caused by the environment. Inaccuracy of some degree is inevitable in all engineering measurements and control. Once encountered, steps can be taken to reduce the sources of error and predictions can be

made of the likelihood of future occurrence. Measures can be taken to reduce and control inaccuracy of measurements during test procedures to eliminate the source, or at least reduce the degree of error. The effects of inaccuracy in measurement should be estimated in advance, before the collection of data, and modifications can be made to the experimental conditions to reduce or eliminate the problem. The likely errors to be found in test results include both measurement and calculation parameters. The uncertainty of measurement parameter can be attributed to the instrument system itself and/or human error, and the uncertainty of calculation parameters results from both parameters. We used Moffat's [14] uncertainty analysis to assess our experiment and the uncertainty of power generation ( $P$ ) was determined to be  $\pm 2.1\%$ .

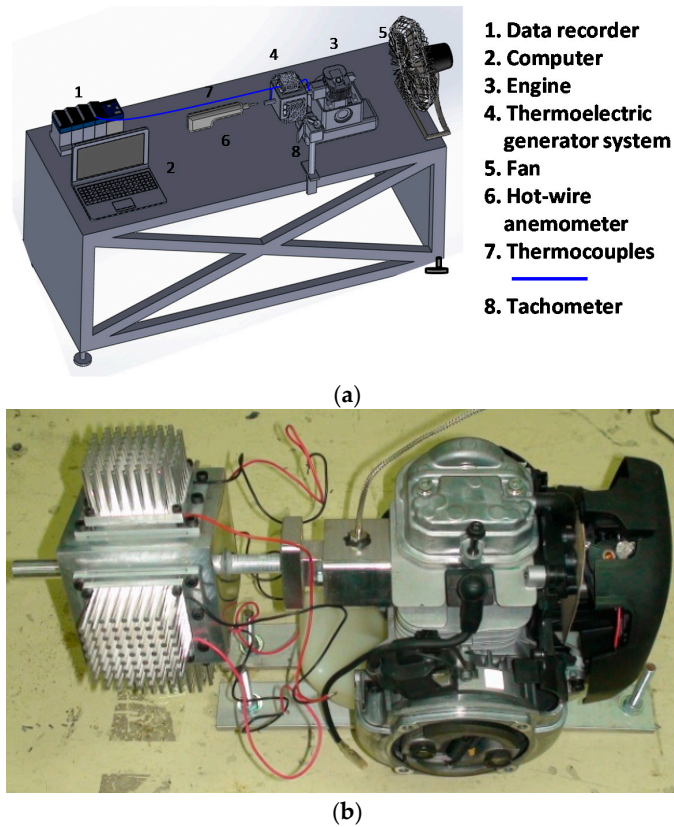


**Figure 6.** The experimental setup of thermoelectric conversion system installed at a real engine. (a) Layout of the experimental equipment; and (b) The 4-stroke engine and the waste heat recovery device.

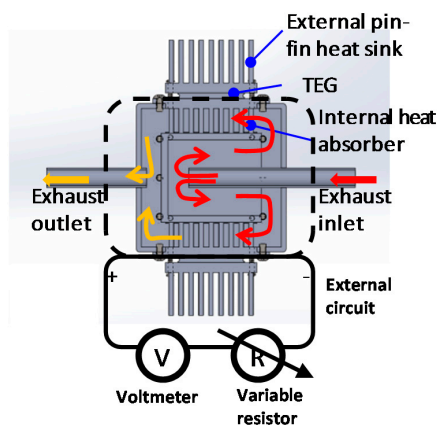


**Figure 7.** Diagram of the thermoelectric conversion system.



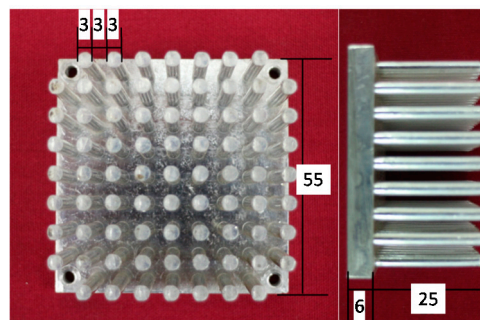


Figure 10. Pin-fin array used in heat sink. (Unit: mm).

### 3. Results and Discussions

#### 3.1. Generation Results of Single-Chip TEG

Figure 11 shows relationship between external load resistor ( $R$ ) and TEG output voltage ( $V$ ). The results show that when temperature difference between hot and cold faces of the TEG is  $\Delta T = T_h - T_c$ , a larger load resistor ( $R$ ) corresponds to a greater TEG output voltage ( $V$ ). TEG voltage resulting from Seebeck effect is the product of Seebeck coefficient multiplied by  $\Delta T$ . Therefore, an increase of the external load resistor ( $R$ ) may also increase the Seebeck coefficient of the TEG. Figure 12 shows the relationship between TEG output voltage ( $V$ ) and output current ( $I$ ). When  $\Delta T$  is constant, the output current ( $I$ ) has an almost linear tendency to decrease with TEG output voltage ( $V$ ). The relationship between the TEG generation power ( $P$ ) and external load resistor ( $R$ ) (see Figure 13) shows that, at the load range of 2–20  $\Omega$ , the maximum TEG generation power output ( $P$ ) is achieved when  $R = 6.8 \Omega$ . Based on the maximum power transfer theory, the maximum power conversion occurs when the external load resistor ( $R$ ) equals the internal resistance ( $r$ ). The internal resistance of the TEG module (TGM-287-1.0-1.5 KRYOTHERM) is about 7  $\Omega$ , which agrees with the present result. Figures 14 and 15 show the relationships between TEG output voltage ( $V$ ) and TEG generation Power ( $P$ ), as well as TEG output voltage ( $V$ ) and generation efficiency ( $\eta$ ). The results show that there exists an optimal output voltage that will yield the maximum generation power ( $P$ ) and efficiency ( $\eta$ ); this voltage corresponds to an external load resistance of 6.8  $\Omega$ , which is closest to the internal resistance of the selected TEG. A maximum output of 2.716 W was achieved when the temperature difference between the hot and cold faces of the TEG was  $\Delta T = T_h - T_c = 120 \text{ }^\circ\text{C}$ , where the optimal generation efficiency ( $\eta$ ) is 3.61%. Figure 16 shows the relationship between temperature difference ( $\Delta T = T_h - T_c$ ) and optimal generation power ( $P_{\max}$ ) when the average temperature of the TEG was 89–117  $^\circ\text{C}$ . This figure also shows that maximum power ( $P_{\max}$ ) increases as the temperature difference between the hot and cold faces of the TEG rises; the reason is that a larger temperature difference between the hot and cold faces results in higher heat transfer rate and output electric voltage. After summarizing all the test results, we could write a correlation regarding maximum generation power ( $P_{\max}$ ) and temperature difference ( $\Delta T = T_h - T_c$ ) between the hot and cold faces of the TEG:  $P_{\max} = 0.0002 \times (T_h - T_c)^2$ . Figure 17 shows the relationship between the average temperature difference ( $\Delta T = T_h - T_c$ ) and  $V/(T_h - T_c)$  when  $\Delta T = T_h - T_c = 80\text{--}120 \text{ }^\circ\text{C}$ . This figure shows that the difference of the Seebeck coefficient ( $S_B - S_A$ ) of the TEG decreases with its average temperature ( $(T_h - T_c)/2$ ). This must be caused by the smaller difference of the TEG Seebeck coefficient ( $S_B - S_A$ ) when its average temperature rises. We also arrived at a correlation regarding the ( $S_B - S_A$ ) of the single-chip TEG used in the experiment and the average temperature of the hot and cold faces:  $S_B - S_A = 0.0708 \times [(T_h + T_c)/2]^{-0.142}$ , within the current range of test temperature, a minor variation of ( $S_B - S_A$ ) is seen, at an approximately constant value of 0.0368.

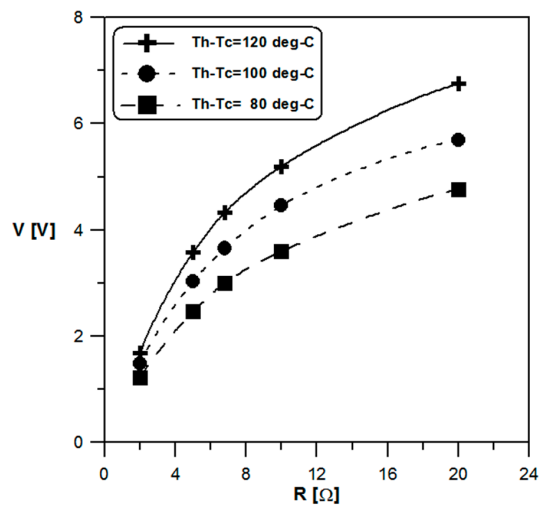


Figure 11. External resistance ( $R$ ) vs. TEG output voltage ( $V$ ).

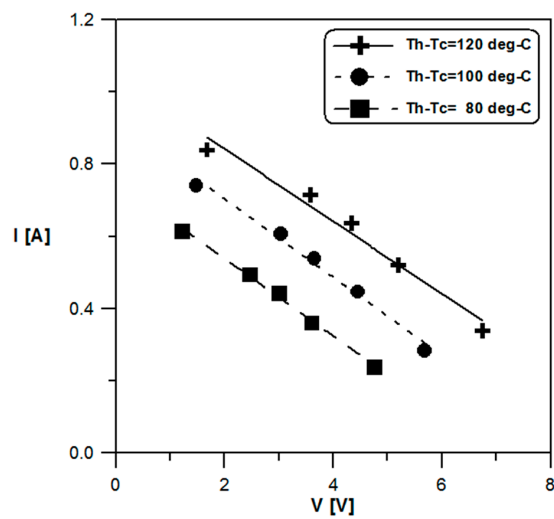


Figure 12. TEG output voltage ( $V$ ) vs. output current ( $I$ ).

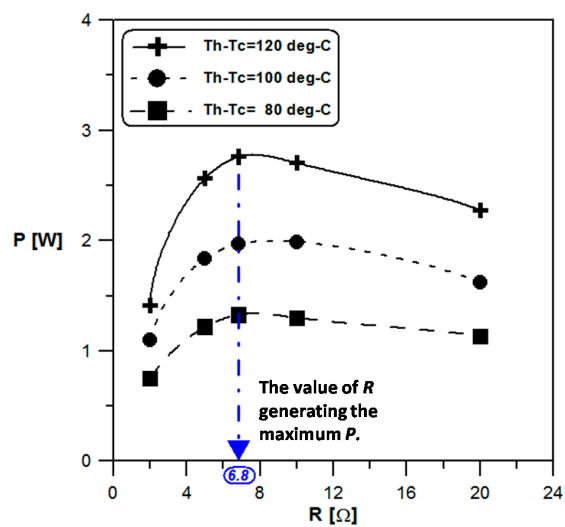


Figure 13. External load resistance ( $R$ ) vs. TEG power generation ( $P$ ).

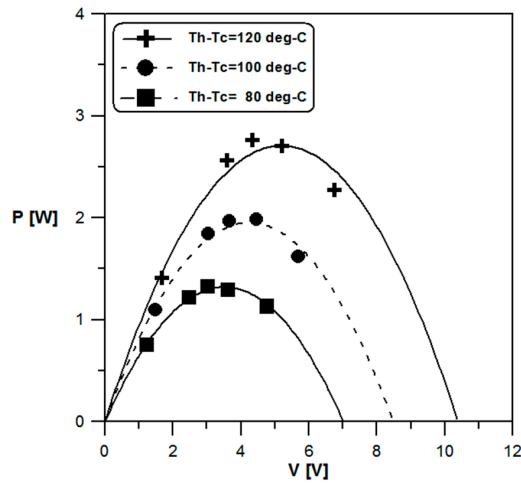


Figure 14. TEG output voltage ( $V$ ) vs. generation power ( $P$ ).

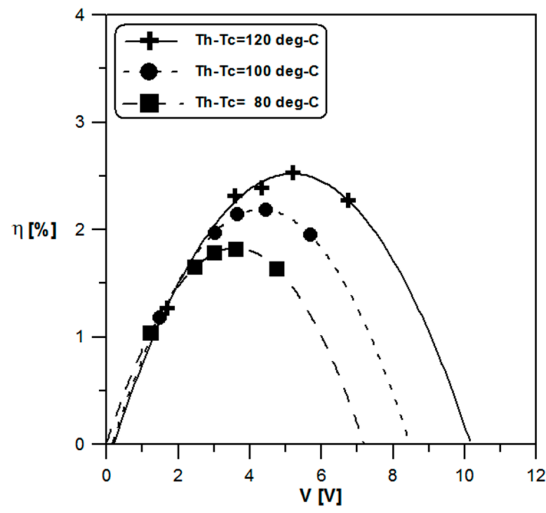


Figure 15. TEG output voltage ( $V$ ) vs. generation efficiency ( $\eta$ ).

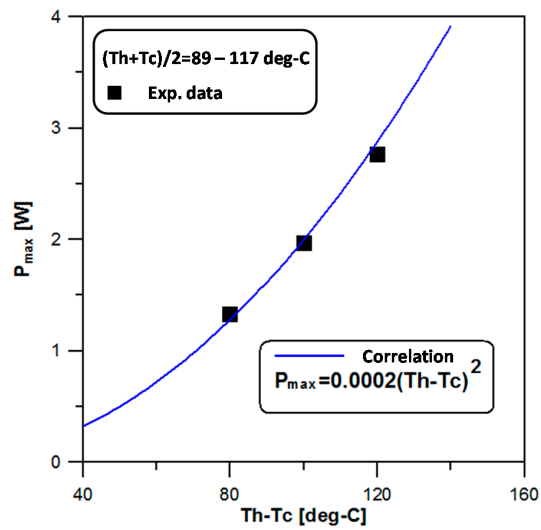


Figure 16. Temperature difference between TEG hot/cold faces ( $T_h - T_c$ ) vs. maximum generation power ( $P_{max}$ ).

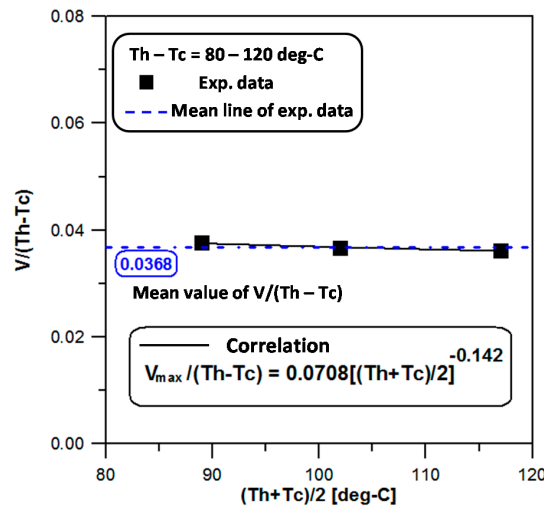


Figure 17. Average TEG temperature  $(T_h - T_c)/2$  vs. Seebeck-coefficient difference  $V/(T_h - T_c)$ .

### 3.2. Generation Results of Thermoelectric Conversion System on a Real Engine

Based on the power transfer theory, the resistance of the load must equal the internal resistance of the voltage source for maximum power transference to the load. Therefore, a variable resistance load system was connected to the output of the TEG to adjust the resistance of the load. The output current and output voltage under different loads was measured and recorded. We calculated the maximum power under different loads, and found that the load resistance that gave the maximum power complied with the internal resistance of the TEG and this was taken as the maximum power.

The main target parameter of the experiment was generation power ( $P$ ). The variable parameters included engine rotation speed ( $\Omega$  [rpm]) and mean velocity ( $U$ ) of air passing through the heat sink, where ( $U$ ) is achieved by adjusting the switch to control the speed of the fan’s motor. The engine speed was controlled by the throttle valve and change in engine speed ( $\Omega$ ) caused the change in the quantity ( $Q_{flow}$ ) of exhaust gas and the temperature ( $T_i$ ) of the exhaust gasses entering the thermoelectric conversion system. Increasing  $Q_{flow}$  and  $T_i$  would increase the hot-side temperature of TEG, promoting the generating performance of TEG. Figure 18 shows the relationship between engine rotation ( $\Omega$ ) and quantity of exhaust gas ( $Q_{flow}$ ). From the near idle ( $\Omega = 2700$  rpm) to the maximum torque output ( $\Omega = 5400$  rpm), the exhaust gas discharge ( $Q_{flow}$ ) was estimated from 500 to 1350 c.c./s.  $Q_{flow}$  increases as  $\Omega$  increases, as shown in Equation (2):

$$Q_{flow} = \Omega \times \frac{1}{60} \times \frac{1}{2} \times (\text{Total displacement}) \times \varphi \tag{2}$$

The total displacement is 35.8 c.c. and the volume efficiency  $\varphi$  is between 0 and 1 and increases with  $\Omega$ . Altering engine rotation speed ( $\Omega$ ) also affects the temperature ( $T_i$ ) of the exhaust gasses entering the thermoelectric conversion system. Since combustion is more efficient at higher engine speed, more combustion heat is generated and the temperature of the exhaust gas goes up when engine speed ( $\Omega$ ) is raised. From Figure 19 it can be seen that an increase in engine speed ( $\Omega$ ) from 2700 to 5400 rpm, results in a change of exhaust gas temperature ( $T_i$ ) from 230 to 325 °C. Additionally, no significant change was seen in the exhaust gas temperature ( $T_i$ ) with the mean cooling air velocity ( $U$ ) used in the experiments. The range of  $U$  may be too small to reveal the influence in  $T_i$ . Furthermore, the 10 cm distance between the engine exhaust outlet and the inlet of the thermoelectric conversion system accounts for a drop of 25–50 °C at the inlet of the thermoelectric conversion system due to heat loss.

During the generation power ( $P$ ) test a voltmeter and a variable resistor are connected in series in the TEG circuit as an external load. The value of the external load resistor ( $R$ ) must be equal to

the internal resistance of the TEG to give the maximum output power. The equation for calculating generation power ( $P$ ) is the same as Equation (1) in Section 2.2.

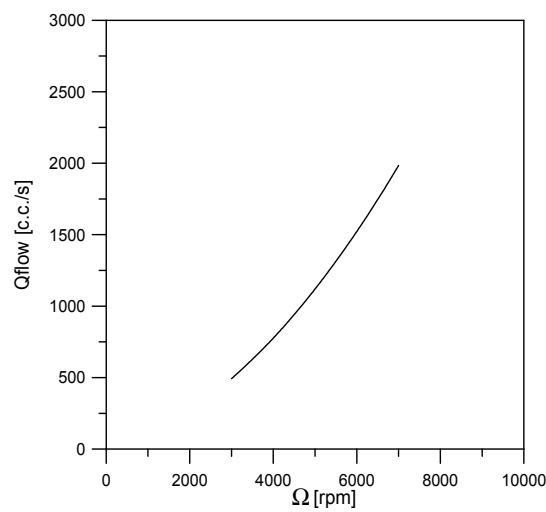


Figure 18. Engine rotation speed ( $\Omega$ ) vs. exhaust gas discharge ( $Q_{flow}$ ).

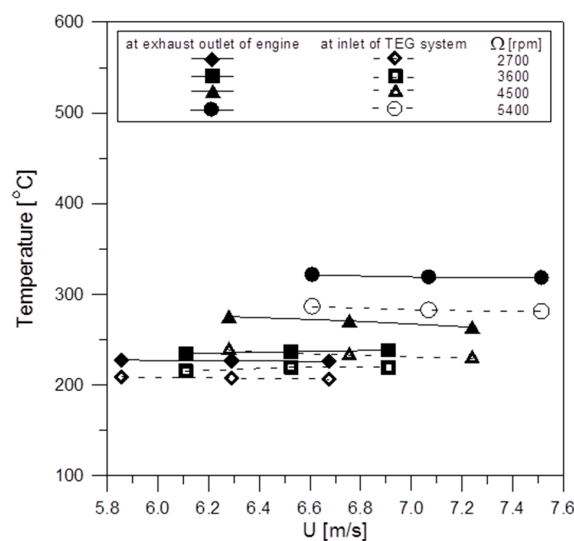


Figure 19. Mean air velocity vs. exhaust temperature.

In this study we used an actual engine to investigate waste heat recovery and the test results are from a specially designed thermoelectric conversion system installed on the exhaust. The variables discussed include the mean velocity ( $U$ ) of air driven by an external fan, the temperature difference ( $\Delta T$ ) between hot/cold faces of the TEGs, the engine rotation speed ( $\Omega$ ) and the quantity ( $Q_{flow}$ ) of exhaust Gas. Figure 20 shows the relationship between the mean air velocity ( $U$ ) and the mean temperature of the TEGs and it can be seen that the mean temperature of the TEGs goes up with an increase in engine rotation speed ( $\Omega$ ). However, no significant change was seen in the mean temperature of the TEGs with the mean air velocity ( $U$ ) used in the experiments. This means that the mean air velocity ( $U$ ) may have been set too low and cooling was insufficient. Furthermore, since the operation temperature of the TEG cannot exceed 200 °C, the engine rotation speed ( $\Omega$ ) in the current study could not cause overheating of the TEGs. Further studies with higher engine rotation speed ( $\Omega$ ) can be conducted in the future. Figure 21 shows the relationship between the mean air velocity ( $U$ ) and the temperature difference ( $\Delta T$ ) of TEGs. Within the current range of the mean velocity ( $U$ ) of air driven by an external

fan, the trend was towards a significant connection between  $\Delta T$  of TEGs and engine rotation speed ( $\Omega$ ). When engine rotation speed ( $\Omega$ ) was increased from 2700 to 5400 rpm,  $\Delta T$  of TEGs increased from 20 to 58 °C.

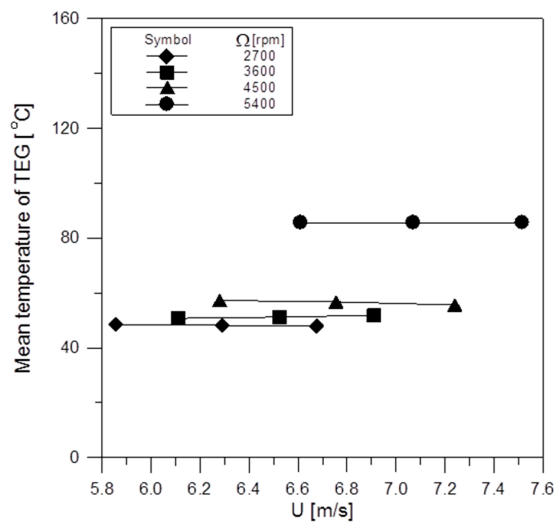


Figure 20. Mean air velocity vs. mean TEG temperature.

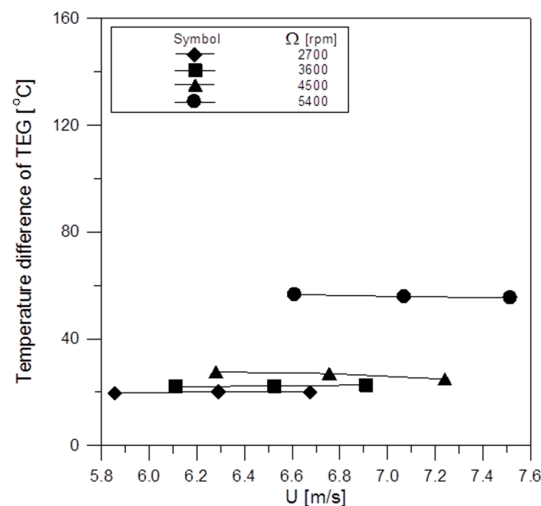


Figure 21. Mean air velocity ( $U$ ) vs.  $\Delta T$  of the TEGs.

From Figure 22 it can be seen that engine rotation speed ( $\Omega$ ) has a significant effect on power generation ( $P$ ) which goes up with an increase of engine rotation speed ( $\Omega$ ). Within the current range of mean air velocity ( $U$ ) used in our experiments, an increase of mean air velocity ( $U$ ) did not increase generated power ( $P$ ). At an engine rotation speed ( $\Omega$ ) of 5400 rpm, the output power ( $P$ ) was 2.5 W. Based on Seebeck thermoelectric generation theory, the TEG output voltage ( $V$ ) satisfies Equation (3):

$$V = \Delta S \cdot \Delta T \tag{3}$$

where  $\Delta S$  is the difference value of the Seebeck coefficient of the semiconductor material used in the TEGs. The value of  $\Delta S$  is not a constant, it varies with temperature of TEGs. However this temperature range is limited as is variation of  $\Delta S$ . A mean value may be used and the generated power ( $P$ ) will equal the square of the produced voltage ( $V$ ) divided by the external resistance ( $R$ ). Our experimental results comply with this assumption. Furthermore, it is predicted that by extending the experimental data to

set the engine rotation speed at 6000 rpm, the output power ( $P$ ) will be 3.8 W. The generated power ( $P$ ) is far below that achieved by the similar thermoelectric conversion system previously designed by the authors where the heat absorber had arrays of straight fins with copper foams in the gaps between fins, and were capable of generating 4.2 W at an engine rotation speed of 6000 rpm. However, the pin-fin array heat absorber used here has lower flow resistance, and the back pressure is not so severe that it would impede normal operation of the engine. Finally, according to the Figure 22, the present system may generate over 5 W when the present small engine (35.8 c.c. displacement) is operating at the maximum power output condition ( $\Omega = 7000$  rpm).

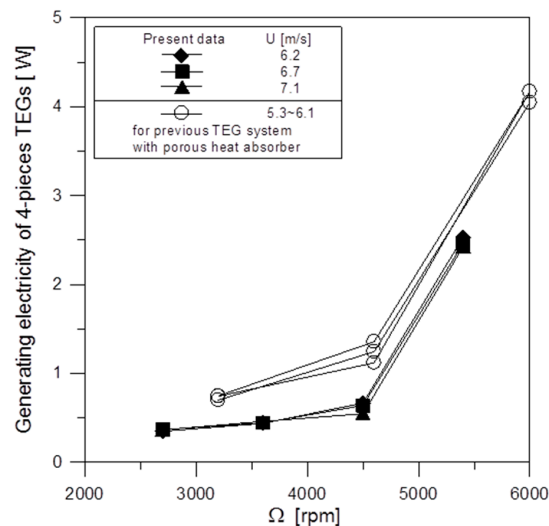


Figure 22. Engine rotation speed ( $\Omega$ ) vs. output power ( $P$ ).

#### 4. Conclusions

An actual four-stroke engine (35.8 c.c.) was used for these experiments on a test platform designed for the investigation of thermoelectric generation using waste heat recovered from the engine exhaust gases. The study successfully investigated the effects of the engine rotation speed and the mean velocity of external cooling air on the temperature and discharged quantity of engine exhaust gas. Experiments were also performed to measure the relationship between the external load resistance and the TEG output voltage/current, as well as between TEG output voltage and generated power/efficiency. A correlation was derived for calculating the maximum generation power of a single-chip TEG and the temperature difference between the hot and cold faces of TEG. The study also examined the influence of engine rotation speed and the velocity of external cooling air against power generation of the thermoelectric conversion system, and found that power generation increased with engine rotation speed. Within the current range of mean velocity of the external cooling air, an increase of cooling-air speed would not increase the generated power. It was found that four TEG modules in series could generate 2.5 W power at an engine rotation speed of 5400 rpm (the maximum torque output). If the present small engine operates at the maximum power output condition ( $\Omega = 7000$  rpm), the present system will generate over 5 W.

**Acknowledgments:** The authors would like to thank the Ministry of Science and Technology of the Republic of China for financially supporting this research under Contract Nos. MOST 104-2221-E-270-005 and MOST 104-2622-E-270-005-CC3.

**Author Contributions:** Tzer-Ming Jeng conducted the experimental measurements and data analysis Sheng-Chung Tzeng led this work and participated discussions; and Bo-Jun Yang and Yi-Chun Li assisted in the implementation of the experimental measurements.

**Conflicts of Interest:** The authors declare no conflict of interest.

## References

1. Champier, D.; Bedecarrats, J.P.; Rivaletto, M.; Strub, F. Thermoelectric power generation from biomass cook stoves. *Energy* **2010**, *35*, 935–942. [[CrossRef](#)]
2. Karri, M.A.; Thacher, E.F.; Helenbrook, B.T. Clarkson Exhaust energy conversion by thermoelectric generator: Two case studies. *Energy Convers. Manag.* **2011**, *52*, 1596–1611. [[CrossRef](#)]
3. Zhou, S.; Sammakia, B.; White, B.; Borgesen, P. Multiscale modeling of thermoelectric generators for the optimized conversion performance. *Int. J. Heat Mass Transf.* **2013**, *62*, 435–444. [[CrossRef](#)]
4. Weng, C.C.; Huang, M.J. A simulation study of automotive waste heat recovery using a thermoelectric power generator. *Int. J. Therm. Sci.* **2013**, *71*, 302–309. [[CrossRef](#)]
5. Jang, J.Y.; Tsai, Y.C. Optimization of thermoelectric generator module spacing and spreader thickness used in a waste heat recovery system. *Appl. Therm. Eng.* **2013**, *51*, 677–689. [[CrossRef](#)]
6. Cummings, T.A. Internal Combustion Electric Power Hybrid Power Plant. U.S. Patent 4,148,192, 23 November 1977.
7. Yoshida, S.; Aoki, K. Thermoelectric Converter for Heat-Exchanger. U.S. Patent 5,959,240, 2 December 1997.
8. Shinohara, K.; Kobayashi, M.; Furuya, K.; Kushibiki, K. Electric Energy Supply System for Vehicle. U.S. Patent 6,172,427, 12 February 1998.
9. Rowe, D.M. Thermoelectrics, an environmentally-friendly source of electrical power. *Renew. Energy* **1999**, *16*, 1251–1256. [[CrossRef](#)]
10. Hendricks, T.J.; Lustbader, J.A. Advanced thermoelectric power system investigations for light-duty and heavy-duty applications. In Proceedings of the 21st International Conference on Thermoelectrics, Long Beach, CA, USA, 25–29 August 2002.
11. Lombardi, C. Researchers Squeeze More Electricity from Heat. Available online: [http://news.cnet.com/8301-17912\\_3-9999450-72.html](http://news.cnet.com/8301-17912_3-9999450-72.html) (accessed on 25 July 2008).
12. Jeng, T.M.; Tzeng, S.C.; Chou, H.C. Experimental study of heat energy absorber with porous medium for thermoelectric conversion system. *Smart Sci.* **2013**, *1*, 1–5.
13. Tzeng, S.C.; Jeng, T.M.; Ma, W.P.; Wang, J.R.; Chou, B.; Lin, J.B.; Xiao, Y.D.; Wu, M.Z.; Tang, F.Z. Exhaust Pipe with Noise-reducing and Heat Recovery Functions. Taiwan, R.O.C. Patent I,350,878, 21 October 2011.
14. Moffat, R.J. Contributions to the theory of single-sample uncertainty analysis. *ASME J. Fluids Eng.* **1982**, *104*, 250–258. [[CrossRef](#)]



© 2016 by the authors; licensee MDPI, Basel, Switzerland. This article is an open access article distributed under the terms and conditions of the Creative Commons by Attribution (CC-BY) license (<http://creativecommons.org/licenses/by/4.0/>).